Disorder and temperature dependence of the anomalous Hall effect in thin ferromagnetic films: Microscopic model

K. A. Muttalib*
Department of Physics, University of Florida, P.O. Box 118440, Gainesville, Florida 32611-8440, USA

P. Wölfle†
ITKM, Universität Karlsruhe, D-76128 Karlsruhe, Germany
and INT, Forschungzentrum Karlsruhe, Postfach 3640, 76021 Karlsruhe, Germany

(Received 23 May 2007; published 19 December 2007)

We consider the anomalous Hall (AH) effect in thin disordered ferromagnetic films. Using a microscopic model of electrons in a random potential of identical impurities including spin-orbit coupling, we develop a general formulation for strong, finite range impurity scattering. Explicit calculations are done within a short range but strong impurity scattering to obtain AH conductivities for both the skew scattering and side-jump mechanisms. We also evaluate quantum corrections due to interactions and weak localization effects. We show that for arbitrary strength of the impurity scattering, the electron-electron interaction correction to the AH conductivity vanishes exactly due to general symmetry reasons. On the other hand, we find that our explicit evaluation of the weak localization corrections within the strong, short-range impurity scattering model can explain the experimentally observed logarithmic temperature dependences in disordered ferromagnetic Fe films.

DOI: 10.1103/PhysRevB.76.214415 PACS number(s): 75.50.Cc, 73.20.Fz, 72.10.Fk, 72.15.Rn

I. INTRODUCTION

It has been recognized since the 1950s (Ref. 1) that a Hall effect can exist in ferromagnetic metals even in the absence of an external magnetic field, hence the name anomalous Hall effect (AHE). There are several different mechanisms that might be responsible for the AHE observed in thin ferromagnetic films, namely, the skew scattering[2] and side-jump mechanisms[3] as well as Berry phase contributions.[4] All such mechanisms depend on the spin-orbit interaction induced by the impurities and on the spontaneous magnetization in a ferromagnet which breaks the time reversal invariance and therefore gives rise to the AHE. For a disordered ferromagnetic film, AH conductivity due to the skew scattering and side-jump mechanisms have been theoretically considered using a variety of methods within weak, short-range impurity scattering.[5–9] However, a systematic calculation, starting from a microscopic Hamiltonian, of the longitudinal as well as the AH conductivities for different mechanisms for strong impurity scattering has been lacking. Recently, the effects of strong, short-range impurity scattering on the longitudinal and Hall conductivities were considered for skew scattering as well as side-jump mechanisms,[10] but quantum corrections, namely, electron-electron (e-e) interaction corrections[11] or weak localization (WL) effects,[12] were not included.

Earlier experiments[13] have shown logarithmic temperature dependences of the longitudinal as well as Hall resistances highlighting the importance of such quantum corrections. However, the results were consistent with, and were interpreted as, vanishing interaction contributions to the AH conductivity, obtained theoretically within a *weak* impurity scattering model[9] and the absence of any weak localization effects. Recent experiments, on the other hand, clearly show a nonvanishing contribution to the total quantum correction to the AH conductivity,[14] which can arise in principle either from an interaction correction due to *strong* impurity scattering or from a weak localization effect, or from a combination of both. It has been commonly believed that weak localization effects in ferromagnetic films would be cut off by the presence of large internal magnetic field among others, which suggests that the interaction corrections to the AH conductivity need to be revisited for strong impurity scattering as a source of difference between the two experiments.

In this paper, we systematically develop a general formulation for the AHE for *strong, finite range* impurity scatterings starting from a microscopic model of electrons in a random potential of impurities including spin-orbit coupling. This generalizes an earlier work[6] which considered weak, short-range impurity scattering only and did not include quantum corrections. We show on very general symmetry grounds that quantum correction to the AH conductivity due to (e-e) interaction effects vanish exactly, which shows that the previous weak scattering results[9] remain valid for arbitrary strengths of the impurity scattering. This forces us to consider the weak localization effects[8] as the only remaining source of the logarithmic temperature dependence in the above experiments despite the presence of large internal magnetic fields and spin-orbit scatterings in these ferromagnetic films. As we show below, the temperature independent cutoff of the weak localization effects in strongly disordered systems can be ineffective at higher temperatures if a temperature dependent contribution dominates the phase relaxation rate. It turns out that while the contribution from the e-e interaction to the phase relaxation rate is indeed too small for WL effects to be observed, a much larger contribution is obtained from scattering off spin waves,[15] which should allow the observation of the WL effects within a reasonable temperature range. We find that the effects of strong impurity scatterings on the WL effects can be evaluated to obtain a very simple result, namely, that the ratio of the WL corrections to the AH to the longitudinal conductivity can be written simply in terms of the eigenvalues of the impurity averaged particle-hole scattering amplitude for zero momentum transfer. This result, taken together with contributions to the AH conductivity from both the skew scattering and side-jump mechanisms calculated within the same microscopic model, can explain both the earlier as well as the recent experiments on the disorder and temperature dependences of the AH conductivities of ultrathin Fe films[14] mentioned above. This last result has been reported without details in combination with the recent experiment in a short letter.[14]

The paper is organized in the following way. A microscopic model Hamiltonian is introduced in Sec. II and a general formulation in two dimensions for strong, finite range impurity scatterings is developed in Sec. III. Section IV reviews the results on the conductivity tensor in the absence of interactions. In Secs. V and VI, we consider the e-e interaction corrections and the weak localization corrections, respectively, to both longitudinal and AH conductivities within the general strong, finite range impurity scattering formulation. We then consider the special case of a short range, but still strong, impurity scattering model in Sec. VII. In Sec. VIII, we collect all the results and compare them with recent experiments. Section IX summarizes the paper. For the sake of completeness, we include models of small and large angle scatterings in the Appendix.

II. HAMILTONIAN

The single particle Hamiltonian of a conduction electron in a ferromagnetic disordered metal, including spin-orbit interaction induced by the disorder potential $V_{dis}(\mathbf{r})$, is given in its simplest form by (throughout the paper, we use units with $\hbar = k_B = 1$)

$$H_1 = \left[-\frac{\nabla^2}{2m} + V_{dis}(\mathbf{r}) \right] \delta_{\sigma\sigma'} - M\tau^z_{\sigma\sigma'} - i\frac{\lambda_c^2}{(4\pi)^2}[\tau_{\sigma\sigma'} \cdot (\nabla V_{dis} \times \nabla)], \tag{2.1}$$

where $\lambda_c = \frac{2\pi}{mc}$ is the Compton wavelength of the electron and M is the Zeeman energy splitting caused by the ferromagnetic polarization. Here, H_1 is a 2×2 matrix in spin space with $\sigma, \sigma' = \uparrow, \downarrow$ being spin indices and τ is the vector of Pauli matrices. The above model is only a crude approximation of the band structure of Fe, which has been determined by several authors (see, e.g., Ref. 16). We model the energy band crossing the Fermi surface by a single isotropic band. As will be discussed below, the quantum corrections to the conductivity exhibit certain qualitative features, which do not depend sensitively on the details of the band structure. The disordered potential in Eq. (2.1) will be modeled as randomly placed identical impurities, $V_{dis}(\mathbf{r}) = \Sigma_j V(\mathbf{r} - \mathbf{R}_j)$. We will later average over the impurity positions $\mathbf{R}_j$.

The matrix elements of H_1 in the plane wave (or Bloch state) representation are given by

$$\begin{aligned}\langle \mathbf{k}'\sigma' | H_1 | \mathbf{k}\sigma \rangle &= \int d^2 r e^{-i\mathbf{k}'\cdot\mathbf{r}} H_1 e^{-i\mathbf{k}\cdot\mathbf{r}} \\ &= \left(\frac{k^2}{2m} - M\sigma \right) \delta_{\mathbf{k}\mathbf{k}'} \delta_{\sigma\sigma'} + \sum_j V(\mathbf{k} - \mathbf{k}') \\ &\quad \times e^{i(\mathbf{k}-\mathbf{k}')\cdot\mathbf{R}_j} + V_{so}(\mathbf{k}'\sigma'; \mathbf{k}\sigma),\end{aligned} \tag{2.2}$$

where $V(\mathbf{k}-\mathbf{k}')$ is the Fourier transform of the single impurity potential and the spin-orbit interaction part is given by

$$V_{so}(\mathbf{k}'\sigma'; \mathbf{k}\sigma) = -i\frac{\lambda_c^2}{(4\pi)^2} \sum_j V(\mathbf{k} - \mathbf{k}') e^{[i(\mathbf{k}-\mathbf{k}')\cdot\mathbf{R}_j]} \tau_{\sigma\sigma'} \cdot (\mathbf{k} \times \mathbf{k}'). \tag{2.3}$$

Here, we have used

$$\begin{aligned}& -i \int d^2 r \exp(-i\mathbf{k}' \cdot \mathbf{r})(\nabla V_{dis} \times \nabla)\exp(-i\mathbf{k}\cdot\mathbf{r}) \\ &= -i \int d^2 r \int \frac{d^2 q}{(2\pi)^2} e^{i(\mathbf{k}-\mathbf{k}'-\mathbf{q})\cdot\mathbf{r}}(-i\mathbf{q})\mathbf{V}(\mathbf{q}) \times (i\mathbf{k}) \\ &= -iV(\mathbf{k}-\mathbf{k}')(\mathbf{k}\times\mathbf{k}').\end{aligned} \tag{2.4}$$

The many-body Hamiltonian is given in terms of electron creation and annihilation operators $c^+_{\mathbf{k}\sigma}, c_{\mathbf{k}\sigma}$ as

$$\begin{aligned}H = \sum_{\mathbf{k}\sigma} (\varepsilon_{\mathbf{k}} - M\sigma) c^+_{\mathbf{k}\sigma} c_{\mathbf{k}\sigma} + \sum_{\mathbf{k}\sigma, \mathbf{k}'\sigma'} \sum_j V(\mathbf{k} - \mathbf{k}') \\ \times e^{i(\mathbf{k}-\mathbf{k}')\cdot\mathbf{R}_j} \{ \delta_{\sigma\sigma'} - i\bar{g}_{so}\tau_{\sigma\sigma'} \cdot (\hat{k} \times \hat{k}') \} c^+_{\mathbf{k}'\sigma'} c_{\mathbf{k}\sigma},\end{aligned} \tag{2.5}$$

where we have defined a dimensionless spin-orbit coupling constant $\bar{g}_{so} \equiv \frac{\lambda_c^2 k_F^2}{(4\pi)^2}$, $\hat{k} \equiv \mathbf{k}/|\mathbf{k}|$. Note: An estimate of the spin-orbit coupling constant $\bar{g}_{so}$, using a typical Fermi wave number k_F, shows that it is rather small, of order 10^{-4}. However, in transition metal compounds, the coupling is substantially enhanced by interband mixing effects,[3] so that the renormalized coupling constant g_{so} is of order unity: $g_{so} \sim c_{so} E_{so}/\Delta E_d$, where $E_{so} \sim 0.1$ eV is a measure for the atomic spin-orbit energy, $\Delta E_d \sim 0.5$ eV is a typical energy splitting of d bands, and the constant $c_{so} \sim 5$. In the following, we will replace $\bar{g}_{so}$ by the phenomenological spin-dependent parameter g_σ.

III. IMPURITY SCATTERING: GENERAL FORMULATION

In this section, we will develop a general formulation for *strong, finite range* impurity scattering in two dimensions using standard field theory techniques at finite temperature.[17] For simplicity, we will need to make approximations for short-range impurity scattering later. However, keeping the formulation general as long as possible will allow us, e.g., to check if the anisotropic scattering can have a large impact on our final results.

The repeated scattering of an electron off a single impurity may be described symbolically in terms of the scattering amplitude $f_{k\sigma,k'\sigma'}$ as

$$f = V + VGV + VGVGV + \cdots, \tag{3.1}$$

where G is the single particle Green's function

$$G_{k\sigma}(i\omega_n) = [i\omega_n - \varepsilon_{k\sigma} - \Sigma_{k\sigma}(\omega_n)]^{-1}, \tag{3.2}$$

with the single particle self-energy $\Sigma_{k\sigma}(i\omega_n)$. Here, $\omega_n = \pi T(2n+1)$ is the fermion Matsubara frequency with T being the temperature and N_σ is the density of states at the Fermi level of spin species σ. (We use units of temperature such that Boltzmann's constant is equal to unity.) V is the bare interaction with one impurity at $\mathbf{R}=\mathbf{0}$ and includes the spin-orbit scattering

$$V_{k,k';\sigma} = V(k-k')[1 - ig_\sigma \tau^z_{\sigma\sigma}(\hat{k}\times\hat{k}')], \tag{3.3}$$

where we have used the fact that V is diagonal in spin space. In the case of finite range, or even long-range correlated scattering potentials, we may still use the model of individual impurities or scattering centers, but now of finite spatial extension. This is reasonable as long as the scattering centers do not overlap too much. If they overlap, a more statistical description in terms of correlators of the impurity potential should be used. Within our model, the nonlocal character of scattering is described in terms of the momentum dependence of the Fourier transform of the potential of a single impurity (assuming only one type of impurity) $V(\mathbf{k}-\mathbf{k}')$, which for an isotropic system depends only on the angle θ between $\mathbf{k}$ and $\mathbf{k}'$, $V=V(\theta)=V(-\theta)$. In two dimensions, we may expand V in terms of eigenfunctions $\chi_m(\hat{k}) = e^{im\phi}$, where ϕ is the polar angle of vector $\mathbf{k}$, $\hat{k}=\mathbf{k}/|\mathbf{k}|$. Adding the skew scattering potential, we may write

$$V_{k,k'\sigma} = \sum_m V_{m\sigma}\chi_m(\hat{k})\chi_m^*(\hat{k}'), \tag{3.4}$$

where $V_{m\sigma}$ is a sum of the normal and skew scattering parts

$$V_{m\sigma} = V_m^{ns} + V_{m\sigma}^{ss}. \tag{3.5}$$

Time reversal invariance and rotation symmetry in the case of potential scattering impliy

$$V_{-m}^{ns} = (V_m^{ns})^* = V_m^{ns}. \tag{3.6}$$

Equation (3.3) then yields

$$V_{m\sigma}^{ss} = \frac{1}{2} g_\sigma \tau^z_{\sigma\sigma}(V_{m-1}^{ns} - V_{m+1}^{ns}). \tag{3.7}$$

A. Scattering amplitude

For V diagonal in spin space, the scattering amplitude $f_{k\sigma,k'\sigma'} = \delta_{\sigma,\sigma'} f_{k,k'\sigma}$ obeys the integral equation

$$\begin{aligned} f^s_{k,k'\sigma} &= V_{k,k'\sigma} + \sum_{k_1} G_{k_1\sigma}(i\omega_n) V_{k,k_1\sigma} f^s_{k_1,k'\sigma} \\ &= V_{k,k'\sigma} - is\pi N_\sigma \langle V_{k,k_1\sigma} f^s_{k_1,k'\sigma}\rangle_{k_1}, \end{aligned} \tag{3.8}$$

where $s \equiv \text{sign}(\omega_n)$ and $\langle\cdots\rangle_{k_1}$ denotes averaging over the direction of wave vector $\mathbf{k}_1$. Defining the dimensionless potential $\bar{V}_{m\sigma} \equiv \pi N_\sigma V_{m\sigma}$ and the dimensionless scattering amplitude $\bar{f}_{k\sigma,k'\sigma'} \equiv \pi N_\sigma f_{k\sigma,k'\sigma'}$ and expanding $\bar{f}_{k\sigma,k'\sigma} = \Sigma_m \bar{f}_{m\sigma}\chi_m(\hat{k})\chi_m^*(\hat{k}')$, we find

$$\bar{f}^s_{m\sigma} = \frac{\bar{V}_{m\sigma}}{1 + is\bar{V}_{m\sigma}}. \tag{3.9}$$

For notational simplicity, we will always use a bar on a symbol to represent the corresponding dimensionless quantity.

B. Single particle relaxation rate

The single particle relaxation rate τ_σ is given by the imaginary part of the self-energy,

$$\frac{1}{2\tau_\sigma} \equiv -s\,\text{Im}\,\Sigma_{k\sigma}(i\omega_n) = -sn_{imp}\,\text{Im}(f^s_{k\sigma,k\sigma}) = \frac{n_{imp}}{\pi N_\sigma}\gamma_\sigma, \tag{3.10}$$

where γ_σ is a dimensionless parameter characterizing the scattering strength, $\gamma_\sigma \equiv -s\Sigma_m\,\text{Im}(\bar{f}_{m\sigma}) = \Sigma_m \frac{\bar{V}^2_{m\sigma}}{1+\bar{V}^2_{m\sigma}}$, and N_σ is the density of states at the Fermi energy of spin species σ. Note that $\bar{V}_{m\sigma}$ are all real.

C. Particle-hole propagator

The particle-hole propagator $\Gamma_{kk'}(q;i\epsilon_n,i\epsilon_n - i\Omega_m)$ is an important ingredient of vertex corrections of any kind. Here, $k+q/2, k-q/2$ are the initial momenta, $k'+q/2, k'-q/2$ the final momenta, and $\epsilon_n, \epsilon_n - \Omega_m$ are the Matsubara frequencies of the particle and the hole lines, respectively. In terms of the particle-hole scattering amplitude $t_{k,k'}(q;i\epsilon_n,i\Omega_m)$, Γ satisfies the following Bethe-Salpeter equation [we have defined dimensionless quantities $\bar{\Gamma}, \bar{t}$ by multiplying both with a factor $(2\pi N_\sigma\tau_\sigma)$]:

$$\begin{aligned} \bar{\Gamma}_{kk'}(q;i\epsilon_n,i\Omega_m) &= \bar{t}_{kk'}(q;i\epsilon_n,i\Omega_m) + (2\pi N_\sigma\tau_\sigma)^{-1} \\ &\quad \times \sum_{k_1} \bar{t}_{kk_1}(q;i\epsilon_n,i\Omega_m) \\ &\quad \times G_{k_1+q/2,\sigma}(i\epsilon_n) G_{k_1-q/2,\sigma}(i\epsilon_n - i\Omega_m) \\ &\quad \times \bar{\Gamma}_{k_1k'}(q;i\epsilon_n,i\Omega_m). \end{aligned} \tag{3.11}$$

The (dimensionless) impurity averaged particle-hole scattering amplitude $\bar{t}$ (we consider only the case of equal spin of particle and hole) is given in terms of the (dimensionless) scattering amplitudes $\bar{f}$ by the equation

$$\begin{aligned} \bar{t}^{ss'}_{kk'}(q;i\epsilon_n,i\Omega_m) &= \frac{2\tau_\sigma n_{imp}}{\pi N_\sigma} \bar{f}^s_{k+q/2,\sigma;k'+q/2\sigma}(i\epsilon_n) \\ &\quad \times \bar{f}^{s'}_{k'-q/2,\sigma;k-q/2,\sigma}(i\epsilon_n - i\Omega_m). \end{aligned} \tag{3.12}$$

We will later need the limit of small $q, q \ll k_F$, of this expression,

$$\bar{t}^{ss'}_{kk'}(q;i\epsilon_n,i\Omega_m) = \bar{t}^{ss'}_{kk'}(q=0) + \Delta\bar{t}^{ss'}_{kk'}(q). \tag{3.13}$$

It is useful to represent the operator $\bar{t}_{kk'}(q=0)$ in terms of its eigenvalues λ_m. Assuming isotropic band structure, the eigenfunctions $\chi_m(\hat{k})=\exp(im\varphi)$ are those of the angular momentum operator component L_z. The eigenvalue equation is

$$\langle \overline{t}_{kk'}(q=0)\chi_m(\hat{k}')\rangle_{k'} = \lambda_m \chi_m(\hat{k}). \tag{3.14}$$

The operator $\overline{t}^{+-}_{kk'}(q=0)$ may be represented as

$$\overline{t}^{+-}_{kk'}(q=0) = \sum_m \lambda_m \chi_m(\hat{k})\chi^*_m(\hat{k}'),$$

$$\overline{t}^{-+}_{kk'}(q=0) = [\overline{t}^{+-}_{k'k}(q=0)]^*. \tag{3.15}$$

In general, using the definitions

$$t^{ss'}_{k,k'\sigma} = \frac{n_{imp}}{(\pi N_\sigma)^2}\overline{f}^s_{k,k'\sigma}\overline{f}^{s'}_{k',k\sigma} = (2\pi N_\sigma \tau_\sigma)^{-1}\overline{t}^{ss'}_{k,k'\sigma},$$

$$\overline{t}^{ss'}_{k,k'\sigma} = \sum_m \overline{t}^{ss'}_{m\sigma}\chi_m(\hat{k})\chi^*_m(\hat{k}'), \tag{3.16}$$

we have

$$\overline{t}^{ss'}_{m\sigma} = \gamma^{-1}_\sigma \sum_{m'} \overline{f}^s_{m'\sigma}\overline{f}^{s'}_{m'-m,\sigma}. \tag{3.17}$$

We will consider $\Delta\overline{t}_{kk'}(q)$ for the special case of strong short-range impurity scatterings in Sec. VII A.

The energy integral over the product of Green's functions in the integral equation for $\Gamma_{kk'}$ may be done first, after expanding the G's in Ω_m and q,

$$\int d\varepsilon_1 G_{k_1+q/2,\sigma}(i\epsilon_n)G_{k_1-q/2,\sigma}(i\epsilon_n - i\Omega_m) = 2\pi\tau[1 + i\tau(i\Omega_m - \mathbf{q}\cdot\mathbf{v}_{k_1}) - \tau^2(\mathbf{q}\cdot\mathbf{v}_{k_1})^2], \tag{3.18}$$

with $\epsilon_n > 0$ and $\epsilon_n - \Omega_m < 0$, where $\mathbf{q}\cdot\mathbf{v}_k = qv_F(\hat{q}\cdot\hat{k})$. Expanding $\overline{\Gamma}_{kk'}$ and $\overline{t}_{kk'}$ in terms of eigenfunctions $\chi_m(\hat{k})$, $\overline{\Gamma}_{kk'} = \Sigma_m \overline{\Gamma}_{mm'}\chi_m(\hat{k})\chi^*_{m'}(\hat{k}')$ and using $\overline{t}^{+-}_{m\sigma} \equiv \lambda_m$, one obtains $(s'=-s)$

$$\begin{aligned}\overline{\Gamma}^{ss'}_{mm'} = \lambda_m\delta_{mm'} + \lambda_m\Bigg\{&[1 - \tau(|\Omega_n| + D_0q^2)]\overline{\Gamma}^{ss'}_{mm'} \\ &- \frac{i}{2}v_Fq\tau s[\overline{\Gamma}^{ss'}_{m-1,m'}\chi^*_1(\hat{q}) + \overline{\Gamma}^{ss'}_{m+1,m'}\chi_1(\hat{q})] \\ &- \frac{1}{4}(v_Fq\tau)^2[\overline{\Gamma}^{ss'}_{m-2,m'}\chi^*_2(\hat{q}) + \overline{\Gamma}^{ss'}_{m+2,m'}\chi_2(\hat{q})]\Bigg\}.\end{aligned} \tag{3.19}$$

For $m=m'\neq 0$, the solution is

$$\overline{\Gamma}_{mm} = \frac{\lambda_m}{1-\lambda_m} + O(q) \equiv \widetilde{\lambda}_m + O(q), \tag{3.20}$$

where we have defined $\widetilde{\lambda}_m \equiv \lambda_m/(1-\lambda_m)$. The λ_m (and therefore $\widetilde{\lambda}_m$) are complex valued and depend on the spin projection σ. Using conventional notation, we will denote the real and imaginary parts of λ_m by λ'_m and λ''_m, respectively, and similarly the real and imaginary parts of $\widetilde{\lambda}_m$ by $\widetilde{\lambda}'_m$ and $\widetilde{\lambda}''_m$, respectively.

The case $m=0$ needs special consideration because particle number conservation causes $\overline{\Gamma}_{00}$ to have a pole in the limit $\Omega_n, q\to 0$, here expressed by $\lambda_0=1$. Solving the above equation for $\overline{\Gamma}_{00}$ in lowest order in q, one finds

$$\overline{\Gamma}_{00} = \frac{1/\tau}{|\Omega_m| + Dq^2}, \tag{3.21}$$

where the renormalized diffusion constant is defined as

$$D = D_0(1+\widetilde{\lambda}'_1), \quad D_0 = \frac{1}{2}v_F^2\tau,$$

$$\widetilde{\lambda}'_1 \equiv \mathrm{Re}\,\widetilde{\lambda}_1 = \frac{1}{2}(\widetilde{\lambda}_1 + \widetilde{\lambda}_{-1}). \tag{3.22}$$

This is found by solving the following equations for small $v_Fq\tau(s'=-s)$:

$$\begin{aligned}\overline{\Gamma}^{ss'}_{00} = 1 + &[1 - \tau(|\Omega_m| + D_0q^2)]\overline{\Gamma}^{ss'}_{00} \\ &- \frac{i}{2}v_Fq\tau s[\overline{\Gamma}^{ss'}_{-1,0}\chi^*_1(\hat{q}) + \overline{\Gamma}^{ss'}_{1,0}\chi_1(\hat{q})],\end{aligned}$$

$$\overline{\Gamma}^{ss'}_{-1,0} = \lambda_{-1}\left[\overline{\Gamma}^{ss'}_{-1,0} - \frac{i}{2}v_Fq\tau s\overline{\Gamma}^{ss'}_{0,0}\chi_1(\hat{q})\right],$$

$$\overline{\Gamma}^{ss'}_{1,0} = \lambda_1\left[\overline{\Gamma}^{ss'}_{1,0} - \frac{i}{2}v_Fq\tau s\overline{\Gamma}^{ss'}_{0,0}\chi_{-1}(\hat{q})\right]. \tag{3.23}$$

Substituting $\overline{\Gamma}^{ss'}_{\pm 1,0}$ into the equation for $\overline{\Gamma}^{ss'}_{00}$, one finds

$$\overline{\Gamma}^{ss'}_{00}\left\{|\Omega_m| + D_0q^2\left[1 + \frac{1}{2}(\widetilde{\lambda}_1 + \widetilde{\lambda}_{-1})\right]\right\} = \frac{1}{\tau}. \tag{3.24}$$

The leading singular dependence on $\hat{k}'$ is obtained from

$$\begin{aligned}\overline{\Gamma}^{ss'}_{0,\pm 1} = &[1 - \tau(|\Omega_m| + D_0q^2)]\overline{\Gamma}^{ss'}_{0,\pm 1} \\ &- \frac{i}{2}v_Fq\tau s[\overline{\Gamma}^{ss'}_{-1,\pm 1}\chi^*_1(\hat{q}) + \overline{\Gamma}^{ss'}_{1,\pm 1}\chi_1(\hat{q})],\end{aligned}$$

$$\overline{\Gamma}^{ss'}_{-1,1} = -\frac{i}{2}\widetilde{\lambda}_{-1}v_Fq\tau s\overline{\Gamma}^{ss'}_{0,1}\chi_1(\hat{q}),$$

$$\overline{\Gamma}^{ss'}_{1,1} = \widetilde{\lambda}_1 - \frac{i}{2}\widetilde{\lambda}_1 v_Fq\tau s\overline{\Gamma}^{ss'}_{0,1}\chi^*_1(\hat{q}). \tag{3.25}$$

The complete particle-hole propagator in the regime $v_Fq\tau < 1$ is given by

$$\overline{\Gamma}_{kk'} = \frac{1}{\tau}\frac{\gamma_k\widetilde{\gamma}_{k'}}{|\Omega_m| + Dq^2} + \sum_{m\neq 0}\widetilde{\lambda}_m\chi_m(\hat{k})\chi^*_m(\hat{k}'), \tag{3.26}$$

with

$$\gamma_k = 1 - \frac{i}{2} v_F q \tau s \sum_{m=\pm1} \tilde{\lambda}_m \chi_m(\hat{k}) \chi m^*(\hat{q})$$
$$= 1 - \frac{i}{2} v_F \tau s \sum_{m=\pm1} \tilde{\lambda}_m \chi_m(\hat{k}) q_{-m} \tag{3.27}$$

and

$$\tilde{\gamma}_k = 1 - \frac{i}{2} v_F \tau s \sum_{m=\pm1} \tilde{\lambda}_m \chi_m^*(\hat{k}) q_m. \tag{3.28}$$

The vertex corrections of the density T_k and current vertices $j_{k\alpha}$ and $\tilde{j}_{k\alpha}$ (for the incoming and outgoing current) are obtained by

$$T_k(q) \equiv 1 + \langle \bar{\Gamma}_{kk'} \rangle_{k'} = 1 + \frac{1/\tau}{|\Omega_m| + Dq^2} \gamma_k \tag{3.29}$$

and

$$j_{k\alpha}(q) = v_{k\alpha} + \langle v_{k'\alpha} \bar{\Gamma}_{k'k} \rangle_{k'}$$
$$= v_{k\alpha} + \sum_{m=\pm1} \tilde{\lambda}_m \chi_m^*(\hat{k}) \langle v_{k'\alpha} \chi_m(\hat{k}') \rangle_{k'}$$
$$+ \langle v_{k'\alpha} \gamma_{k'} \rangle_{k'} \frac{1/\tau}{|\Omega_m| + Dq^2} \tilde{\gamma}_k,$$

$$\tilde{j}_{k\alpha}(q) = v_{k\alpha} + \langle v_{k'\alpha} \bar{\Gamma}_{kk'} \rangle_{k'}$$
$$= v_{k\alpha} + \sum_{m=\pm1} \tilde{\lambda}_m \chi_m(\hat{k}) \langle v_{k'\alpha} \chi_m^*(\hat{k}') \rangle_{k'}$$
$$+ \langle v_{k'\alpha} \tilde{\gamma}_k \rangle_{k'} \frac{1/\tau}{|\Omega_m| + Dq^2} \gamma_k. \tag{3.30}$$

Note that $\tilde{j}_{k\alpha} \neq (j_{k\alpha})^*$, as the eigenvalues $\tilde{\lambda}_m$ are in general complex valued. Using

$$\chi_{-1}(\hat{k}) \chi_1^*(\hat{k}') + \chi_1(\hat{k}) \chi_{-1}^*(\hat{k}') = 2(\hat{k} \cdot \hat{k}'),$$
$$\chi_{-1}(\hat{k}) \chi_1^*(\hat{k}') - \chi_1(\hat{k}) \chi_{-1}^*(\hat{k}') = 2i(\hat{k} \times \hat{k}') \tag{3.31}$$

and

$$\langle \hat{k}'_\alpha (\hat{k} \cdot \hat{k}') \rangle = \frac{1}{2} \hat{k}_\alpha, \quad \langle \hat{k}'_\alpha (\hat{k} \times \hat{k}') \rangle = -\frac{1}{2} (\hat{e}_\alpha \times \hat{k}) \tag{3.32}$$

and defining $j_{k\alpha} \equiv j_{k\alpha}(q=0)$, $\tilde{j}_{k\alpha} \equiv \tilde{j}_{k\alpha}(q=0)$, we have

$$j_{k\alpha} = v_F[(1 + \tilde{\lambda}_1')\hat{k}_\alpha + \tilde{\lambda}_1''(\hat{e}_\alpha \times \hat{k})_z],$$
$$\tilde{j}_{k\alpha} = v_F[(1 + \tilde{\lambda}_1')\hat{k}_\alpha - \tilde{\lambda}_1''(\hat{e}_\alpha \times \hat{k})_z]. \tag{3.33}$$

More explicitly, for $\alpha = x, y$, the incoming and outgoing current vertices j and $\tilde{j}$ have the forms

$$j_{kx} = v_F[(1 + \tilde{\lambda}_1')\hat{k}_x + \tilde{\lambda}_1''\hat{k}_y] = \frac{1}{2} v_F[(1 + \tilde{\lambda}_1^*)\hat{k}_+ + (1 + \tilde{\lambda}_1)\hat{k}_-],$$

$$j_{ky} = v_F[(1 + \tilde{\lambda}_1')\hat{k}_y - \tilde{\lambda}_1''\hat{k}_x] = -i\frac{1}{2} v_F[(1 + \tilde{\lambda}_1^*)\hat{k}_+ - (1 + \tilde{\lambda}_1)\hat{k}_-],$$

$$\tilde{j}_{kx} = v_F[(1 + \tilde{\lambda}_1')\hat{k}_x - \tilde{\lambda}_1''\hat{k}_y] = \frac{1}{2} v_F[(1 + \tilde{\lambda}_1)\hat{k}_+ + (1 + \tilde{\lambda}_1^*)\hat{k}_-],$$

$$\tilde{j}_{ky} = v_F[(1 + \tilde{\lambda}_1')\hat{k}_y + \tilde{\lambda}_1''\hat{k}_x] = -i\frac{1}{2} v_F[(1 + \tilde{\lambda}_1)\hat{k}_+ - (1 + \tilde{\lambda}_1^*)\hat{k}_-], \tag{3.34}$$

where we have defined $k_\pm = k_x \pm i k_y$.

D. Particle-particle propagator

The integral equation for the particle-particle propagator or Cooperon reads (again multiplying the Cooperon C and the particle-particle scattering amplitude t^p by the factor $2\pi N_\sigma \tau_\sigma$ to define dimensionless Cooperon $\bar{C}$ and dimensionless particle-particle scattering amplitude $\bar{t}^p$)

$$\bar{C}_{kk'}(Q; i\epsilon_n, i\Omega_m) = \bar{t}^p_{kk'}(Q; i\epsilon_n, i\Omega_m)$$
$$+ (2\pi N_\sigma \tau_\sigma)^{-1} \sum_{k_1} \bar{t}^p_{kk_1}(Q; i\epsilon_n, i\Omega_m) G_{k_1,\sigma}(i\epsilon_n)$$
$$\times G_{Q-k_1,\sigma}(i\epsilon_n - i\Omega_m) \bar{C}_{k_1 k'}(q; i\epsilon_n, i\Omega_m), \tag{3.35}$$

$$t^{p,ss'}_{k,k'\sigma} = \frac{n_{imp}}{(\pi N_\sigma)^2} \bar{f}^s_{k,k'\sigma} \bar{f}^{s'}_{-k,-k',\sigma} = (2\pi N_\sigma \tau_\sigma)^{-1} \gamma_\sigma^{-1} \bar{f}^s_{k,k'\sigma} \bar{f}^{s'}_{-k,-k',\sigma}, \tag{3.36}$$

$$\bar{t}^{p,ss'}_{k,k'\sigma} = 2\pi N_\sigma \tau_\sigma t^{p,ss'}_{k,k'\sigma} = \sum_m \bar{t}^{p,ss'}_{m\sigma} \chi_m(\hat{k}) \chi_m^*(\hat{k}'), \tag{3.37}$$

$$\bar{t}^{p,ss'}_{m\sigma} = \gamma_\sigma^{-1} \sum_{m'} \bar{f}^s_{m'\sigma} \bar{f}^{s'}_{m-m',\sigma}. \tag{3.38}$$

If rotation invariance or time reversal invariance is broken, $\bar{t}^{p,ss'}_{0\sigma} = \gamma_\sigma^{-1} \gamma^p_\sigma \neq 1$, where $\gamma^p_\sigma = \Sigma_{m'} \bar{f}^s_{m'\sigma} \bar{f}^{s'}_{-m',\sigma}$.

The energy integral over the product of Green's functions in the integral equation for $C_{kk'}$ may be done first, after expanding the G's in Ω_m and Q,

$$\int d\varepsilon_1 G_{k_1,\sigma}(i\epsilon_n) G_{Q-k_1,\sigma}(i\epsilon_n - i\Omega_m)$$
$$= 2\pi\tau[1 + i\tau(i\Omega_m - \mathbf{Q} \cdot \mathbf{v}_{k_1}) - \tau^2(\mathbf{Q} \cdot \mathbf{v}_{k_1})^2], \tag{3.39}$$

with $\epsilon_n > 0$, $\epsilon_n - \Omega_m < 0$, where $\mathbf{Q} \cdot \mathbf{v}_k = Q v_F (\hat{Q} \cdot \hat{k})$. Expanding $\bar{C}_{kk'}$ and $\bar{t}^p_{kk'}$ in terms of eigenfunctions $\chi_m(\hat{k})$, $\bar{C}_{kk'} = \Sigma_m \bar{C}_{mm'} \chi_m(\hat{k}) \chi_{m'}^*(\hat{k}')$ and denoting $\bar{t}^{p,+-}_{m\sigma} = \lambda^p_m$, one obtains $(s' = -s)$

$$\bar{C}_{mm'} = \lambda_m^p \Bigg\{ \delta_{mm'} + [1 - \tau(|\Omega_n| + D_0 Q^2)]\bar{C}_{mm'} - \frac{i}{2} v_F Q \tau [\bar{C}_{m-1,m'} \chi_1^*(\hat{Q}) + \bar{C}_{m+1,m'} \chi_1(\hat{Q})] - \frac{1}{4}(v_F Q \tau)^2 [\bar{C}_{m-2,m'} \chi_2^*(\hat{Q}) + \bar{C}_{m+2,m'} \chi_2(\hat{Q})] \Bigg\}. \quad (3.40)$$

The $m=m'=0$ component of $\bar{C}_{mm'}$ obeys the equation

$$[(\tau_\varphi^{so})^{-1} + |\Omega_n| + D_0 Q^2]\widetilde{C}_{00} = \tau^{-1} - \frac{i}{2} v_F Q [\bar{C}_{-1,0} \chi_1^*(\hat{Q}) + \bar{C}_{1,0} \chi_1(\hat{Q})] + O(Q^2), \quad (3.41)$$

where $(\tau_\varphi^{so})^{-1}$ is the phase relaxation rate contributed by spin-orbit interaction processes,

$$(\tau_\varphi^{so})^{-1} = \tau^{-1}[(\lambda_0^p)^{-1} - 1]. \quad (3.42)$$

Using

$$\bar{C}_{\pm 1,0} = \lambda_{\pm 1}^p \left[\bar{C}_{\pm 1,0} - \frac{i}{2} v_F Q \tau \bar{C}_{0,0} \chi_{\pm 1}(\hat{q}) \right], \quad (3.43)$$

the Cooperon is found as

$$\bar{C}_{kk'} = \frac{1}{\tau} \frac{\gamma_k^p \widetilde{\gamma}_{k'}^p}{|\Omega_m| + D^p Q^2 + \tau_\varphi^{-1}} + \sum_{m \neq 0} \widetilde{\lambda}_m^p \chi_m(\hat{k}) \chi_m^*(\hat{k}'),$$

$$\widetilde{\lambda}_m^p = \frac{\lambda_m^p}{1 - \lambda_m^p}, \quad (3.44)$$

with

$$\gamma_k^p = 1 - \frac{i}{2} v_F Q \tau \sum_{m=\pm 1} \widetilde{\lambda}_m^p \chi_m(\hat{k}) \chi_m^*(\hat{Q}) = 1 - i\tau \sum_{m=\pm 1} \widetilde{\lambda}_m^p \chi_m(\hat{k}) \langle \mathbf{Q} \cdot \mathbf{v}_{k'} \chi_m^*(\hat{k}') \rangle \quad (3.45)$$

and

$$\widetilde{\gamma}_k^p = 1 - i\tau s \sum_{m=\pm 1} \widetilde{\lambda}_m^p \chi_m^*(\hat{k}) \langle \mathbf{q} \cdot \mathbf{v}_{k'} \chi_m(\hat{k}') \rangle. \quad (3.46)$$

Here, the diffusion coefficient D^p is in general different from the one in the p-h channel,

$$D^p = D_0 \left[1 + \frac{1}{2}(\widetilde{\lambda}_1^p + \widetilde{\lambda}_{-1}^p) \right] \neq D, \quad (3.47)$$

the difference being proportional to the spin-orbit coupling g_σ.

IV. CONDUCTIVITY TENSOR IN THE ABSENCE OF INTERACTION

As mentioned before, there are three mechanisms contributing to the anomalous Hall conductivity, namely, the skew scattering, the side-jump, and the Berry phase mechanisms. In this section, we will write down the generic formulations for evaluating these contributions within the diagrammatic perturbation theory. The contribution to the conductivity $\sigma_{\alpha\beta}$ will be given in terms of a correlation function $L_{\alpha\beta}$, defined as[17]

$$\sigma_{\alpha\beta} = e^2 \sum_{\Omega \to 0} \lim \frac{1}{i\Omega_m} L_{\alpha\beta}, \quad (4.1)$$

where $L_{\alpha\beta} = \sum_n L_{\alpha\beta}^{d_n}$ is a sum of the different relevant diagrams d_n. We will take the current to be along the x direction, so the longitudinal conductivity will correspond to $\alpha=\beta=x$, while the (anomalous) Hall conductivity will be given by the off-diagonal part $\alpha=x$, $\beta=y$. Note that $\sigma_{yx} = -\sigma_{xy}$.

A. Skew scattering contribution

The skew scattering contribution to the conductivity tensor $\sigma_{\alpha\beta}$ in lowest order in $1/\varepsilon_F \tau$ is given by the bubble diagram dressed by vertex corrections given by the correlation function

$$L_{\alpha\beta} = T \sum_{\epsilon_n} \sum_{k,\sigma} G_{k\sigma}(i\epsilon_n) G_{k\sigma}(i\epsilon_n - i\Omega_m) v_{k\alpha} \widetilde{j}_{k\beta}^\sigma. \quad (4.2)$$

The energy integration over GG is nonzero only if the poles are on opposite sides of the real axis, requiring $0 \leq \epsilon_n \leq \Omega_m$ (we assume $\Omega_m > 0$), and yields $2\pi N_\sigma \tau_\sigma$, and the summation on ϵ_n gives $\Omega_m/(2\pi T)$. Substituting $\widetilde{j}_{k\beta}^\sigma$ from Eq. (3.34) into the Kubo formula, the conductivity tensor follows as

$$\sigma_{\alpha\beta}^{ss} = \sum_\sigma \frac{1}{2} v_F^2 \tau_\sigma N_\sigma \begin{pmatrix} 1 + \widetilde{\lambda}_1' & \widetilde{\lambda}_1'' \\ -\widetilde{\lambda}_1'' & 1 + \widetilde{\lambda}_1' \end{pmatrix}. \quad (4.3)$$

Defining the tensor of diffusion coefficients $D_{\alpha\beta}^\sigma$ as

$$D_{\alpha\alpha}^\sigma = \frac{1}{2} v_F^2 \tau_\sigma^{tr},$$

$$D_{xy}^\sigma = D_{\alpha\alpha}^\sigma [\widetilde{\lambda}_1''/(1 + \widetilde{\lambda}_1')] = -D_{yx}^\sigma, \quad (4.4)$$

where

$$\tau_\sigma^{tr} \equiv \tau_\sigma (1 + \widetilde{\lambda}_1') \quad (4.5)$$

is the momentum relaxation time, we may write

$$\sigma_{\alpha\beta}^{ss} = \sum_\sigma N_\sigma D_{\alpha\beta}^\sigma. \quad (4.6)$$

From the definition $\widetilde{\lambda}_m = \lambda_m/(1-\lambda_m)$, we obtain the following identities:

$$1 + \widetilde{\lambda}_1 = \frac{1}{1 - \lambda_1}, \quad 1 + \widetilde{\lambda}_1' = \frac{1 - \lambda_1'}{|1 - \lambda_1|^2}, \quad \widetilde{\lambda}_1'' = \frac{\lambda_1''}{|1 - \lambda_1|^2}. \quad (4.7)$$

B. Side-jump contribution

The side-jump contribution has been first calculated by Berger.[3] It arises because the trajectory of a wave packet

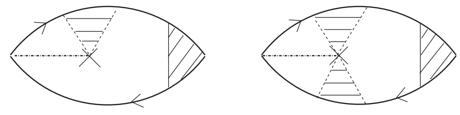

FIG. 1. Diagrams for side-jump contributions. Solid lines are impurity averaged Green's functions. Shaded triangles with dashed lines represent impurity scattering amplitudes while the dotted line from a vertex denotes spin-orbit term in the velocity operator. The shaded vertex represents vertex corrections to the current density operator.

scattered by an impurity is shifted sidewise due to the spin-orbit interaction ("side jump"). This effect may be calculated in a straightforward way[18] by observing that the side jump leads to an additional term in the particle velocity due to the spin-orbit interaction. Indeed, the quantum mechanical velocity obtained from the Heisenberg equation of motion for the position operator has two terms,

$$\mathbf{v} = \frac{d}{dt}\mathbf{r} = -i[\mathbf{r},H_1] = \frac{\mathbf{p}}{m} + \frac{1}{4m^2c^2}(\tau \times \nabla V_{dis}). \tag{4.8}$$

The Bloch state matrix elements of $\mathbf{v}$ are given by

$$\langle \mathbf{k}'\sigma' |\mathbf{v}|\mathbf{k}\sigma\rangle = \frac{\mathbf{k}}{m}\delta_{\mathbf{kk}'}\delta_{\sigma\sigma'} - i\frac{g_\sigma}{2m\varepsilon_F}\sum_j V(\mathbf{k}-\mathbf{k}') \times e^{i(\mathbf{k}-\mathbf{k}')\cdot\mathbf{R}_j}\{\tau_{\sigma\sigma'} \times (\mathbf{k}-\mathbf{k}')\}. \tag{4.9}$$

For strong impurity scattering, there are six diagrams that contribute to the current correlation function, four of type (a) and two of type (b), shown in Fig. 1. For example, contributions from diagrams of Figs. 1(a) and 1(b) give

$$L_{xy}^{1a} = -in_{imp}\frac{g}{\epsilon_F}T\sum_{\mathbf{kk}'} V^2 G_k^+ G_{k'}^+ G_k^- \left[\tau \times \frac{\mathbf{k}-\mathbf{k}'}{2m}\right]_x f_{k'k}^+ \tilde{j}_{k_y},$$

$$L_{xy}^{1b} = -in_{imp}\frac{g}{\epsilon_F}T\sum_{\mathbf{kk}'} V^2 G_{k'}^+ G_{k_1}^+ G_{k_1}^- G_k^- \left[\tau \times \frac{\mathbf{k}-\mathbf{k}'}{2m}\right]_x \times f_{k'k_1}^+ f_{k_1k}^- \tilde{j}_{k_{1y}}. \tag{4.10}$$

These were evaluated within the short-range strong impurity scattering model in Ref. 10. We will later use the results reported there.

C. Berry phase contribution

In general, Berry phase contributions can arise when there is an anomalous velocity term, as in the case of the side-jump contribution given by Eq. (4.8). In principle, such terms can also arise in the presence of a periodic potential and spin-orbit interaction leading to finite Berry curvatures.[4] It has been found that the intrinsic Berry curvature contributions to the AH conductivity for bulk ferromagnetic metals can be large in magnitude.[19] Analogous contributions for thin film ferromagnets have not been obtained yet. Such contributions depend on the details of the band structure and are beyond the scope of the present work. On the other hand, the focus of the current work is on the disorder and temperature dependence of the AH conductivity in which the Berry contributions are qualitatively similar to the side-jump contributions (both arise from an additional velocity term due to spin-orbit interactions). Therefore, the effects of Berry contributions can be included in a phenomenological way, while comparing with experiments, by considering a larger side-jump contribution to the total AH conductivity.

V. INTERACTION CORRECTIONS TO THE CONDUCTIVITY

The e-e interaction corrections to the conductivity will be calculated in first order in the screened Coulomb interaction. It may therefore be represented as an integral over a kernel $K(q,i\omega_l)$ multiplied by the screened Coulomb interaction $V_c(q,i\omega_l)$,

$$\delta\sigma^I = T\sum_{\omega_l}\int dq^2 K(q,i\omega_l)V_c(q,i\omega_l). \tag{5.1}$$

Gauge invariance requires that $\delta\sigma$ should be invariant against an energy shift of the interaction potential, $V(\mathbf{r}) \to V(\mathbf{r})+C$, which only leads to a constant term in the total Hamiltonian. In Fourier space, the transformation is $V(\mathbf{q}) \to V(\mathbf{q})+\mathbf{C}\delta(\mathbf{q})$, which requires the kernel to vanish in the limit $\mathbf{q}\to 0$.[20] [Even more general, since $V(\mathbf{q})$ is an electric potential, a gauge transformation of the above form, but with arbitrary time dependence $C=C(t)$, does not change the physical fields.] We will see below that this gauge invariance, together with an additional mirror symmetry, will impose a strong constraint on the interaction corrections to the Hall conductivity.

A. Coulomb interaction renormalized by diffusion

The Coulomb interaction $V_c(q,\omega_l)$ is renormalized by diffusion processes. The bare screened interaction is given by

$$V_c(q,i\omega_l) = V_B(q)/[1 + V_B(q)\Pi(q,i\omega_l)], \tag{5.2}$$

where $V_B(q)=4\pi e^2/q^2$ in three dimensions and $V_B(q)=2\pi e^2/q$ in two dimensions, and the polarization function is given by[12]

$$\Pi(q,i\omega_l) = \frac{dn}{d\mu}\frac{Dq^2}{|\omega_l| + Dq^2}. \tag{5.3}$$

In two dimensions, one therefore finds

$$V_c(q,i\omega_l) = \frac{2\pi e^2}{q}\frac{|\omega_l| + Dq^2}{|\omega_l| + Dq^2 + DqK_2} \to \left(\frac{dn}{d\mu}\right)^{-1}, \tag{5.4}$$

in the limit $\omega_l=0$, $q\to 0$. Note that in a ferromagnet, an additional effective electron-electron interaction arises by exchange of spin-wave excitations. We do not consider this interaction here because it is small, of order $(J/\epsilon_F)^2$, where J is the exchange energy (see Sec. VI B).

B. Singular contributions for skew scattering

The diagrams for the correlation functions $L_{\alpha\beta}$ defined in Eq. (4.1) can have up to three diffusion poles.[21] The gauge

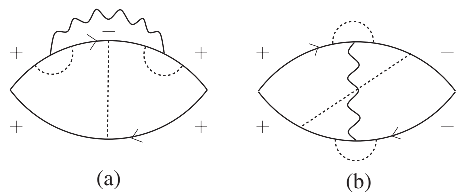

FIG. 2. Diagrams for interaction corrections. Solid lines are impurity averaged Green's functions, wavy lines denote screened Coulomb interactions, and dashed lines denote diffusion poles. There are two diagrams of type (a) and two of type (b).

invariance argument presented above suggests that the relevant contributions to $K(q,i\omega_l)$ should have a factor of q^2, which cancels one of the diffusion poles. Therefore, only diagrams with three diffusion poles shown in Fig. 2 contribute. For example, contribution from diagram (a) of Fig. 2 is given by

$$\begin{aligned}L^{2a}_{\alpha\beta} = &- T\sum_{\epsilon_n} T\sum_{\omega_l} \sum_{\mathbf{k},\mathbf{k}',\mathbf{q}} G^2_k(\epsilon_n) G_{k-q}(\epsilon-\omega)\\ &\times G_{k'-q}(\epsilon-\omega) G_{k'}(\epsilon_n) G_{k'}(\epsilon_n-\Omega)\\ &\times V(\mathbf{q},\omega_l)[\Theta(\epsilon)\Theta(\Omega)\Theta(\omega-\epsilon)\\ &\times T^{+-}_k(\mathbf{q},\omega) T^{-+}_{k'}(-\mathbf{q},-\omega)\Gamma^{+-}_{k'k}(\mathbf{q},\omega-\Omega)\\ &+\Theta(-\epsilon)\Theta(\Omega-\epsilon)\Theta(\epsilon-\omega) T^{-+}_k(\mathbf{q},\omega)\\ &\times T^{+-}_{k'}(-\mathbf{q},-\omega)\Gamma^{+-}_{kk'}(-\mathbf{q},\omega+\Omega)] v_{k\alpha} v_{k'\beta}. \end{aligned} \quad (5.5)$$

Using only the singular parts

$$\Gamma^{+-}_{kk'}(\mathbf{q},\Omega) = \frac{\gamma_k(\mathbf{q})\tilde{\gamma}_{k'}(\mathbf{q})}{|\Omega| + Dq^2},$$

$$\Gamma^{-+}_{kk'}(\mathbf{q},\omega) = \Gamma^{+-}_{k'k}(-\mathbf{q},-\omega) \quad (5.6)$$

and

$$T^{+-}_k(\mathbf{q},\omega) = \frac{\gamma_k(\mathbf{q})}{|\omega| + Dq^2}, \quad T^{-+}_k(\mathbf{q},\omega) = \frac{\tilde{\gamma}_k(-\mathbf{q},)}{|\omega| + Dq^2} \quad (5.7)$$

and defining

$$\mathcal{D}_q(\omega_l,\Omega_m) = \frac{V(q,\omega_l)}{(|\omega_l| + Dq^2)^2(|\omega_l-\Omega_m| + Dq^2)}, \quad (5.8)$$

one gets

$$\begin{aligned}L^{2a}_{\alpha\beta} = \sum_\sigma (-2\pi i N_0\tau^2)^2 \sum_{\mathbf{q}} \Bigg[& T\sum_{\omega_l>\Omega_m} (\omega_l - \Omega_m)\\ &\times \langle v_{k\alpha}\gamma_k(\mathbf{q})\tilde{\gamma}_k(\mathbf{q})\xi_k(\mathbf{q})\rangle_k \langle v_{k'\beta}\tilde{\gamma}_{k'}(\mathbf{q})\gamma_{k'}(\mathbf{q})\xi_{k'}(\mathbf{q})\rangle_{k'}\\ &+ T\sum_{\omega_l<0} |\omega_l| \langle v_{k\alpha}\tilde{\gamma}_k(-\mathbf{q})\gamma_k(-\mathbf{q})\xi^*_k(\mathbf{q})\rangle_k\\ &\times \langle v_{k'\beta}\gamma_{k'}(-\mathbf{q})\tilde{\gamma}_{k'}(-\mathbf{q})\xi^*_{k'}(-\mathbf{q})\rangle_{k'}\Bigg]\frac{1}{2\pi}\mathcal{D}_{\mathbf{q}}(\omega_l,\Omega_m), \end{aligned} \quad (5.9)$$

where we have expanded the Green's functions for small q and defined the factor

$$\xi_k \equiv 1 - 2i\tau(\mathbf{q}\cdot\mathbf{v_k}). \quad (5.10)$$

Note that $\tilde{\gamma}_k(-\mathbf{q},-\Omega) = \tilde{\gamma}_k(\mathbf{q},\Omega)$. The leading terms in q are the linear in q terms in the products $\gamma\tilde{\gamma}\xi$,

$$\begin{aligned}&\gamma_k(\pm\mathbf{q})\tilde{\gamma}_k(\pm\mathbf{q})\xi_k(\mathbf{q})\\ &\quad = 1 \mp 2i\tau(\mathbf{q}\cdot\mathbf{v_k}) \mp \frac{i}{2} v_F\tau \sum_{m=\pm1} [\tilde{\lambda}_m + \tilde{\lambda}^*_m]\chi_m(\hat{k}) q_{-m}. \end{aligned} \quad (5.11)$$

The $\tilde{\lambda}$'s combine to $\tilde{\lambda}'_m = \tilde{\lambda}'_{-m}$, which may be pulled in front of the m summation. Observe that

$$v_F \sum_{m=\pm1} \chi_m(\hat{k}) q_{-m} = 2(\mathbf{q}\cdot\mathbf{v_k}). \quad (5.12)$$

Therefore, quite generally,

$$\langle v_{kx}\gamma_k(\mathbf{q})\tilde{\gamma}_k(\mathbf{q})\xi_k(\mathbf{q})\rangle_k = -i v_F^2 \tau q_x (1 + \tilde{\lambda}'_1). \quad (5.13)$$

C. Corrections to longitudinal conductivity within skew scattering model

For contributions from diagram (a) of Fig. 2 to the longitudinal conductivity, each of the two angular averages (in each term) in Eq. (5.9) with $\alpha=\beta=x$ gives a factor proportional to q_x [see Eq. (5.13)], the product yielding q_x^2. Diagram (b) also has the same combination. This yields, for the four diagrams (a), (a′), (b), and (b′), the total contribution ($L^{2a}_{xx} = L^{2a'}_{xx}$; $L^{2b}_{xx} = L^{2b'}_{xx}$),

$$\begin{aligned}&L^{2a+2a'+2b+2b'}_{xx}\\ &\quad = \frac{1}{2\pi}\sum_\sigma (2\pi N_\sigma \tau^2)^2 (v_F^2\tau)^2 (1+\tilde{\lambda}'_1)^2 \sum_{\mathbf{q}} q^2 \Psi(q,\Omega_m), \end{aligned} \quad (5.14)$$

where we have defined

$$\begin{aligned}\Psi(q,\Omega_m) &= T\sum_{\omega_l>0} \omega_l [\mathcal{D}(-\omega_l,\Omega_m) - \mathcal{D}(-\omega_l-\Omega_m,\Omega_m)]\\ &= T\left[\sum_{0<\omega_l<\Omega_m} \omega_l + \sum_{\omega_l>\Omega_m} \Omega_m\right]\mathcal{D}(-\omega_l,\Omega_m). \end{aligned} \quad (5.15)$$

The sum over q converted to an integral yields

$$\sum_{\mathbf{q}} q^2 \Psi(q,\Omega_m) = \frac{1}{4\pi}\frac{e^2}{D^2\kappa}\Omega\left(1 + \ln\frac{\omega_c}{2\pi T}\right), \quad (5.16)$$

where $\kappa \equiv 2\pi e^2 \Sigma_\sigma N_\sigma$ is the screening length.

The exchange interaction correction to the longitudinal conductivity is then given by

$$\delta\sigma^{ex}_{xx} = \frac{e^2}{\Omega_m} L_{xx} = -\frac{e^2}{2\pi^2}\ln\frac{\omega_c}{T}, \quad (5.17)$$

where we used $D_\sigma = D_{0\sigma}(1+\tilde{\lambda}'_{1\sigma})$. Note that the correction $\delta\sigma_{xx}$ is independent of the scattering strength.

D. Corrections to Hall conductivity within skew scattering model

For $\alpha=x$, $\beta=y$, the two angular averages in Eq. (5.9) are proportional to q_x and q_y, respectively, so that the angular q integral yields zero. This is true for all four diagrams (a), (a′), (b), and b′. Thus, the total correction to the Hall conductivity L_{xy} within the skew scattering model is zero. Note that the results are true for arbitrary strength as well as finite range and anisotropy of the impurity scattering.

Note that the result that the angular average [Eq. (5.13)] is proportional to q_x is a special consequence of the fact that Eq. (5.9) contains the combination $\gamma_k\tilde{\gamma}_k$. This particular combination is proportional to $\mathbf{q}\cdot\mathbf{v_k}$, as shown in Eq. (5.12), which results in Eq. (5.13). This is true for the class of diagrams considered here. This leads to the obvious question if there are other diagrams where the angular average is over a different combination of γ_k's leading to a nonzero contribution to L_{xy}. It turns out that, indeed, there are such terms with less than three diffusion poles, but that there is a deeper reason why the *total* interaction correction to the Hall conductivity must always vanish in the first order in Coulomb interaction. In this case, the interaction correction has the form Eq. (5.1) and the kernel must be proportional to q^2 as mentioned before. In addition, we have the following symmetry properties for the Hall conductivity with respect to a sign change of the magnetization (magnetic field) and a mirror reflection from the yz plane $x\rightarrow -x$ (or from the xz plane $y\rightarrow -y$), which follow from the invariance of the Hamiltonian under a simultaneous transformation $B\rightarrow -B$ and $x\rightarrow -x$ (or $y\rightarrow -y$),

$$\sigma_{xy}(B) = -\sigma_{xy}(-B),$$

$$\sigma_{xy}(B;x) = \sigma_{xy}(-B;-x) = -\sigma_{xy}(B;-x), \qquad (5.18)$$

which means that the Kernel must be proportional to q_xq_y to preserve the mirror symmetry. Thus, even though individual diagrams do contribute, the total sum of all diagrams of a given class must cancel to yield vanishing contribution to the Hall conductivity. Note that the above argument remains valid for the side-jump contributions as well. Therefore, we have, quite generally,

$$\delta\sigma^I_{xy} = 0. \qquad (5.19)$$

This generalizes the results of Ref. 9 where this result was first obtained within a skew scattering model with short-range and weak impurity scattering.

Note that the above arguments do not imply that the weak localization correction to the Hall conductivity must also vanish because the WL contributions do not have the form Eq. (5.1) and the gauge invariance arguments do not apply.

E. Corrections to conductivity within side-jump model

We have already argued that the e-e interaction corrections to the Hall conductivity due to side-jump scattering must vanish on very general symmetry grounds. The corresponding corrections to the longitudinal conductivity are of course finite. However, these contributions are proportional to the spin-orbit coupling and therefore are much smaller than the corrections due to normal scattering obtained above. We will therefore neglect such contributions.

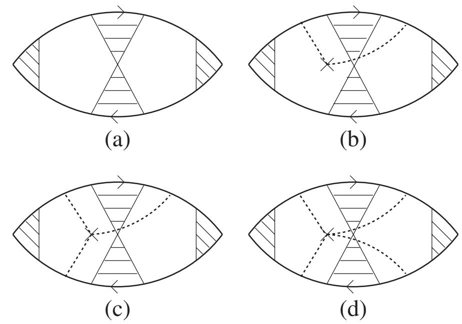

FIG. 3. Diagrams for weak localization corrections. Solid lines are impurity averaged Green's functions and broken lines are impurity scattering amplitudes. Shaded cross is the Cooperon and shaded vertices are vertex corrections to the current density operator. There are two diagrams of type (b) and four diagrams of type (c).

F. Hartree terms

Equation (5.17) should be corrected by including diagrams of the Hartree type. This leads to the total interaction correction in two dimensions,[11]

$$\delta\sigma^I_{xx} = -\frac{e^2}{2\pi^2}\left(1-\frac{3}{4}\tilde{F}_\sigma\right)\ln\frac{\omega_c}{T}, \qquad (5.20)$$

where

$$\tilde{F}_\sigma = 8(1+F/2)\ln(1+F/2)/F - 4 \qquad (5.21)$$

and

$$F = \frac{1}{v(q=0)}\int\frac{d\theta}{2\pi}v(q=2k_F\sin\theta/2). \qquad (5.22)$$

As we will discuss later, experiments suggest an approximate cancellation between the exchange and Hartree terms, which will imply that the quantity

$$h_{xx} \equiv \left(1-\frac{3}{4}\tilde{F}\right) \qquad (5.23)$$

can be very small.

VI. WEAK LOCALIZATION CORRECTION TO CONDUCTIVITY

As pointed out before, the weak localization contributions cannot be written as an integral over a kernel, as in Eq. (5.1) for the Coulomb interaction. Therefore, although the mirror symmetry is still preserved, the total contribution to the Hall conductivity need not be zero.

A. Cooperon contributions

The weak localization correction to the current-current correlator is obtained from diagrams shown in Fig. 3, with one Cooperon propagator connecting the upper and lower lines of the conductivity bubble. The frequency arguments of the upper (particle) line and the lower (hole) line have opposite signs. The current vertices are dressed. For example, the contribution of diagram (a) of Fig. 3 to the current correlation function is

$$L_{\alpha\beta}^{3a}=\sum_{\sigma}T\sum_{\epsilon_n}\sum_{\mathbf{k},\mathbf{k}',\mathbf{Q}}G_{k\sigma}(i\epsilon_n)G_{k\sigma}(i\epsilon_n-i\Omega_m)G_{k'\sigma}(i\epsilon_n)\times G_{k'\sigma}(i\epsilon_n-i\Omega_m)j_{k\alpha}^{\sigma}\tilde{j}_{k'\beta}^{\sigma}(2\pi N_\sigma\tau_\sigma)^{-1}\bar{C}_{kk'}(\mathbf{Q};i\epsilon_n,i\Omega_m). \tag{6.1}$$

Here, the momentum $\mathbf{Q}=\mathbf{k}+\mathbf{k}'$ can be taken to be small, as for $Q\to 0$ the Cooperon is strongly peaked. Consequently, one may take $\mathbf{k}'\approx-\mathbf{k}$ in the arguments of the Green's functions and of the current vertex, i.e., $\tilde{j}_{k'\beta}^{\sigma}\approx-\tilde{j}_{k\beta}^{\sigma}$. Then,

$$L_{\alpha\beta}^{3a}=-(\Omega_m/2\pi)\sum_{\sigma}(4\pi N_\sigma\tau_\sigma^3)\times(2\pi N_\sigma\tau_\sigma)^{-1}\langle j_{k\alpha}^{\sigma}\tilde{j}_{k\beta}^{\sigma}\rangle_k\sum_{\mathbf{Q}}\bar{C}_{k,-k}(\mathbf{Q}). \tag{6.2}$$

The Cooperon contribution is given by

$$\Phi\equiv\sum_{\mathbf{Q}}\bar{C}_{k,-k}(\mathbf{Q})=\int_0^{Q_c}\frac{QdQ}{2\pi}\frac{1/\tau}{|\Omega_m|+D^pQ^2+\tau_\varphi^{-1}}=(4\pi\tau_\sigma D^p)^{-1}\ln(\tau_\varphi/\tau_\sigma), \tag{6.3}$$

leading to a logarithmic temperature dependence through $\tau_\varphi(T)$. Similarly, contributions from the two diagrams of type (b) can be evaluated to give

$$\begin{aligned}L_{\alpha\beta}^{3b}&=n_{imp}\sum_{\sigma}T\sum_{\epsilon_n}\left\{\sum_{\mathbf{k}}[G_{k\sigma}(i\epsilon_n)]^2G_{k\sigma}(i\epsilon_n-i\Omega_m)\right\}^2\times j_{k\alpha}^{\sigma}\tilde{j}_{k\beta}^{\sigma}f_{k,-k'\sigma}^{+}f_{-k,k'\sigma}^{+}\Phi\\&=n_{imp}\frac{\Omega_m}{2\pi}\sum_{\sigma}(-2\pi iN_\sigma\tau_\sigma^2)^2(2\pi N_\sigma\tau_\sigma)^{-1}\times(\pi N_\sigma)^{-2}\langle j_{k\alpha}^{\sigma}\tilde{j}_{k\beta}^{\sigma}\bar{f}_{k,-k'\sigma}^{+}\bar{f}_{-k,k'\sigma}^{+}\rangle_k\Phi,\end{aligned}$$

$$L_{\alpha\beta}^{3b'}=n_{imp}\frac{\Omega_m}{2\pi}\sum_{\sigma}(2\pi iN_\sigma\tau_\sigma^2)^2(2\pi N_\sigma\tau_\sigma)^{-1}\times(\pi N_\sigma)^{-2}\langle j_{k\alpha}^{\sigma}\tilde{j}_{k\beta}^{\sigma}\bar{f}_{k',-k\sigma}^{-}\bar{f}_{-k',k\sigma}^{-}\rangle_k\Phi, \tag{6.4}$$

so that

$$L_{\alpha\beta}^{3b+3b'}=n_{imp}\frac{\Omega_m}{2\pi}\sum_{\sigma}(-2\pi iN_\sigma\tau_\sigma^2)^2(2\pi N_\sigma\tau_\sigma)^{-1}\times(\pi N_\sigma)^{-2}(v_F^2\gamma_\sigma)^{-1}\times\Phi\langle j_{k\alpha}^{\sigma}\tilde{j}_{k'\beta}^{\sigma}[\bar{f}_{k,-k'\sigma}^{+}\bar{f}_{-k,k'\sigma}^{+}+\bar{f}_{k',-k\sigma}^{-}\bar{f}_{-k',k\sigma}^{-}]\rangle_k. \tag{6.5}$$

In a similar fashion, the total contributions from all diagrams can then be written as

$$L_{\alpha\beta}^{WL}=-\frac{\Omega_m}{4\pi^2}\sum_{\sigma}(D_\sigma/D_\sigma^p)J^{\alpha\beta}\ln(\tau_\varphi/\tau_\sigma),$$

$$J^{\alpha\beta}=J_1^{\alpha\beta}+J_2^{\alpha\beta}+4iJ_3^{\alpha\beta}-4J_5^{\alpha\beta}, \tag{6.6}$$

where

$$J_1^{\alpha\beta}=\frac{2}{v_{F\sigma}^2}\langle j_{k\alpha}^{\sigma}\tilde{j}_{k\beta}^{\sigma}\rangle,$$

$$J_2^{\alpha\beta}=(v_F^2\gamma_\sigma)^{-1}\langle j_{k\alpha}^{\sigma}\tilde{j}_{k'\beta}^{\sigma}[\bar{f}_{k,-k'\sigma}^{+}\bar{f}_{-k,k'\sigma}^{+}+\bar{f}_{k',-k\sigma}^{-}\bar{f}_{-k',k\sigma}^{-}]\rangle_k,$$

$$J_3^{\alpha\beta}=(v_F^2\gamma_\sigma)^{-1}\langle j_{k\alpha}^{\sigma}\tilde{j}_{k'\beta}^{\sigma}[\bar{f}_{k,-k'\sigma}^{+}\bar{f}_{-k_1,k'\sigma}^{+}\bar{f}_{k_1,k\sigma}^{-}-\bar{f}_{-k',k\sigma}^{-}\bar{f}_{k',-k_1\sigma}^{-}\bar{f}_{k,k_1\sigma}^{+}]\rangle_{k,k',k_1},$$

$$J_5^{\alpha\beta}=(v_F^2\gamma_\sigma)^{-1}\langle j_{k\alpha}^{\sigma}\tilde{j}_{k'\beta}^{\sigma}\bar{f}_{k,k_2\sigma}^{+}\bar{f}_{-k_1,k'\sigma}^{+}\bar{f}_{k',-k_2\sigma}^{-}\bar{f}_{k_1,k\sigma}^{-}\rangle_{k,k',k_1,k_2}. \tag{6.7}$$

Here, $J_1^{\alpha\beta}$ corresponds to the contribution from diagram (a) of Fig. 3, $J_2^{\alpha\beta}$ is a sum of contributions from the two diagrams of type (b), $J_3^{\alpha\beta}$ is a sum of contributions from two diagrams of type (c) [the other two of type (c) gives $J_4^{\alpha\beta}=J_3^{\alpha\beta}$], and $J_5^{\alpha\beta}$ is a contribution from diagram (d). In the above, we have used the relation $(n_{imp}/\pi N_\sigma)=1/(2\gamma_\sigma\tau_\sigma)$.

B. Phase relaxation rate

The Cooperon contribution depends on the phase relaxation rate τ_φ^{-1}, which grows linearly with temperature T. In general, this may be cut off by spin-flip scattering τ_s, by spin-orbit scattering τ_{so}, or by a magnetic field characterized by ω_H, all of which are independent of temperature. Therefore, a logarithmic temperature dependence in the conductivity requires that the phase relaxation rate satisfies the inequality

$$\max(1/\tau_s,1/\tau_{so},\omega_H)\ll 1/\tau_\varphi\ll 1/\tau_{tr}. \tag{6.8}$$

The contribution to τ_ϕ from e-e interaction is given by

$$1/\tau_\varphi=\frac{T}{\epsilon_F\tau_{tr}}\ln\frac{\epsilon_F\tau_{tr}}{2}. \tag{6.9}$$

This is typically too small to satisfy the above inequality in thin ferromagnetic films where, in particular, the internal magnetic field B_{in} can be estimated to give rise to $\omega_H=4(\epsilon_F\tau_{tr})(eB_{in}/m^*c)$ which can be large. A much larger contribution is obtained from scattering off spin waves in such systems,[15] which is given by

$$1/\tau_\varphi=4\pi T\frac{J^2}{\epsilon_F\Delta_g}, \tag{6.10}$$

where J is the exchange energy of the s electrons and Δ_g is the spin-wave gap. As estimated in Ref. 14, with this contribution to the phase relaxation rate, the inequality [Eq. (6.8)] can be satisfied within experimentally accessible disorder and temperature ranges where the WL effects can be observed.

VII. STRONG SHORT-RANGE IMPURITY SCATTERING

The results of the previous section can in principle be used to obtain the weak localization corrections to both longitudinal and Hall conductivities. However, the algebra gets fairly involved without contributing extra insight into the problem. Since higher angular momentum components are expected to be smaller, we will consider the dominant contribution that arises from a short-range impurity model and show in the Appendix how effects of finite range anisotropic scattering can be included within model calculations. On the other hand, we will keep the calculations valid for arbitrary strength of the impurity scattering.

A. Scattering amplitude, relaxation rate, and particle-hole and particle-particle propagators

These were already obtained for short-range strong impurity scatterings in Ref. 10 and we will simply quote the results. The scattering amplitude is given by

$$\bar{f}_{k\sigma,k'\sigma'} = \frac{\tilde{w}}{\sqrt{w}} - i\tau^z_{\sigma\sigma}(\hat{k}\times\hat{k}')\frac{2\tilde{u}}{\sqrt{u}} - is_{\omega_n}[\tilde{w} + 2\tilde{u}(\hat{k}\cdot\hat{k}')]. \tag{7.1}$$

Here, we defined $\tilde{w}=w/(1+w)$ and $\tilde{u}=u/(1+u)$, where $w=(\pi N_\sigma V)^2$ and $u=(g_\sigma/2)^2 w$, and all quantities depend on the spin orientation σ (suppressed here and in the following, except in the final expressions involving spin summation). In terms of the angular momentum components of $\bar{f}$ defined in Eq. (3.9), $\bar{f}^s_m$, we have from Eq. (7.1),

$$\bar{f}^s_{kk'} = \bar{f}^s_0 + \bar{f}^s_1\hat{k}_+\hat{k}'_- + \bar{f}^s_{-1}\hat{k}_-\hat{k}'_+, \quad \bar{f}^s_0 = \frac{\tilde{w}}{\sqrt{w}} - is\tilde{w},$$

$$\bar{f}^s_{\pm1} = -is\tilde{u} \pm \tau^z_{\sigma\sigma}\frac{\tilde{u}}{\sqrt{u}}, \quad \bar{f}^s_m = 0, \quad |m| > 1. \tag{7.2}$$

Using Eq. (7.2), the single particle relaxation rate given by Eq. (3.10) becomes

$$\frac{1}{2\tau_\sigma} = \frac{n_{imp}}{\pi N_\sigma}(\tilde{w} + 2\tilde{u}). \tag{7.3}$$

One observes that $\frac{1}{2\tau_\sigma}$ is proportional to the Fermi energy, the average number of impurities per electron, and the dimensionless factor $(\tilde{w}+2\tilde{u})$, expressing the effective scattering strength per impurity. Eigenvalues of the particle-hole scattering amplitude $\bar{t}^{+-}_{kk'}$ are obtained to be

$$\lambda_0 = 1, \quad \lambda_{-m} = \lambda^*_m,$$

$$\lambda_1 = 2\tilde{w}\tilde{u}(\tilde{w} + 2\tilde{u})^{-1}\left(1 + is\frac{1}{\sqrt{u}}\tau^z_{\sigma\sigma}\right),$$

$$\lambda_2 = \frac{\tilde{u}^2}{u}(\tilde{w} + 2\tilde{u})^{-1}(u - 1 + 2is\sqrt{u}\tau^z_{\sigma\sigma}), \tag{7.4}$$

while for $\bar{t}^{++}_{kk'}$ one obtains [with $\bar{t}^{ss}_{kk'} \equiv \Sigma_m \xi_m \chi_m(\hat{k})\chi^*_m(\hat{k}')$]

$$\xi_0 = (\tilde{w} + 2\tilde{u})^{-1}\left[\frac{\tilde{w}}{1+w}(1 - w - 2is\sqrt{w}) + 2\tilde{u}\frac{1-u}{1+u}\right],$$

$$\xi_1 = -2\tilde{w}\tilde{u}(\tilde{w} + 2\tilde{u})^{-1}\left(1 + is\frac{1}{\sqrt{w}}\right),$$

$$\xi_2 = -\tilde{u}(\tilde{w} + 2\tilde{u})^{-1}. \tag{7.5}$$

It may be shown that $\Delta\bar{t}_{kk'}(q)$ defined in Eq. (3.13) gives rise to small corrections to the diffusion coefficient, of order $(1/\varepsilon_F\tau)$, and hence may be dropped.

Eigenvalues of the particle-particle scattering amplitude $\bar{t}^{p,+-}_{kk'}$ are obtained to be

$$\lambda^p_0 = [\tilde{w} - 2\tilde{u}(1 - 2\tilde{u})]/(\tilde{w} + 2\tilde{u}),$$

$$\lambda^p_{\pm1} = \left(2\tilde{w}\tilde{u} \pm 2\frac{\tilde{w}}{\sqrt{w}}\frac{\tilde{u}}{\sqrt{u}}\tau^z_{\sigma\sigma}\right) \Big/ (\tilde{w} + 2\tilde{u}),$$

$$\lambda^p_{\pm2} = \tilde{u}/(\tilde{w} + 2\tilde{u}). \tag{7.6}$$

We observe that $\lambda^p_0 \neq 1$ if skew scattering is present, as it violates time reversal symmetry.

The phase relaxation rate $(\tau^{so}_\varphi)^{-1}$ defined in Eq. (3.42) is given by

$$(\tau^{so}_\varphi)^{-1} = \tau^{-1}4\tilde{u}(1 - \tilde{u})/[\tilde{w} - 2\tilde{u}(1 - 2\tilde{u})], \tag{7.7}$$

which is positive for not too large spin-orbit scattering, $u \lesssim w/2$ or $g_\sigma \lesssim 1$.

B. Hall conductivity

The conductivity tensor due to skew scattering was already evaluated in Sec. IV A for general strong finite range impurity scattering in terms of the eigenvalues of the particle-hole propagator λ. In particular, it gives

$$\frac{\sigma^{ss}_{xy}}{\sigma^{ss}_{xx}} = \frac{\lambda''_1}{1 - \lambda'_1}. \tag{7.8}$$

For short-range scattering, Eq. (7.4) gives explicit expressions for the eigenvalues in terms of the scattering potentials. The side-jump contribution was already evaluated in Ref. 10 and we quote the result,

$$\sigma^{sj}_{xy} = \frac{e^2}{2\pi}\sum_\sigma \tau^z_{\sigma\sigma}g_\sigma\frac{\tilde{w}}{\tilde{w} + 2\tilde{u}}\frac{(1 + \tilde{\lambda}'_1)}{1 + u} \tag{7.9}$$

Using Eq. (7.4), this yields, in the small $u \ll w \ll 1$ limit,

$$\sigma^{sj}_{xy} = \frac{e^2}{2\pi}\sum_\sigma \tau^z_{\sigma\sigma}g_\sigma\frac{1}{1 - \lambda'_1}. \tag{7.10}$$

C. Weak localization correction

Evaluation of $J^{\alpha\beta}$ defined in Sec. VI [Eqs. (6.6) and (6.7)] in the present short-range (but arbitrary scattering strength) model gives

$$J_1^{xx}=(1+\tilde{\lambda}_1')^2-(\tilde{\lambda}_1'')^2, \quad J_1^{xy}=2\tilde{\lambda}_1''(1+\tilde{\lambda}_1'),$$

$$J_2^{xx}=[\lambda_1'J_1^{xx}-\lambda_1''J_1^{xy}], \quad J_2^{xy}=[\lambda_1''J_1^{xx}+\lambda_1'J_1^{xy}],$$

$$J_3^{xx}=\frac{i}{2}[2\tilde{u}\lambda_1'J_1^{xx}-(2\tilde{u}+1)\lambda_1''J_1^{xy}],$$

$$J_3^{xy}=\frac{i}{2}[(2\tilde{u}+1)\lambda_1''J_1^{xx}+2\tilde{u}\lambda_1'J_1^{xy}],$$

$$J_5^{xx}=-\frac{1}{2}[(2\tilde{u}-1)\lambda_1'J_1^{xx}-2\tilde{u}\lambda_1''J_1^{xy}],$$

$$J_5^{xy}=-\frac{1}{2}[2\tilde{u}\lambda_1''J_1^{xx}+(2\tilde{u}-1)\lambda_1'J_1^{xy}],$$

$$iJ_3^{\alpha\beta}-J_5^{\alpha\beta}=-\frac{1}{2}J_2^{\alpha\beta}, \quad J^{\alpha\beta}=J_1^{\alpha\beta}-J_2^{\alpha\beta}. \tag{7.11}$$

We may combine this into the compact expression

$$J^{xx}=\mathrm{Re}\{\Lambda\}, \quad J^{xy}=\mathrm{Im}\{\Lambda\}, \quad \Lambda=\frac{1}{1-\lambda_1}. \tag{7.12}$$

Note that the final result for $J^{\alpha\beta}$ contains detailed effects of the potentials only through the eigenvalues λ. This suggests that the results may be more general than the short-range potentials used in the calculations. Also, as we will show in the Appendix, λ_1' may approach unity in the limit of extreme forward scattering.

In any case, for the short-range impurity scattering model considered above, we then have contributions from weak localization corrections given by

$$\delta\sigma_{xx}^{WL}=-\frac{e^2}{4\pi^2}\sum_\sigma (D_\sigma/D^p)\ln(\tau_\varphi/\tau_\sigma),$$

$$\frac{\delta\sigma_{xy}^{WL}}{\delta\sigma_{xx}^{WL}}=\frac{\mathrm{Im}(\Lambda)}{\mathrm{Re}(\Lambda)}=\frac{\lambda_1''}{1-\lambda_1'}. \tag{7.13}$$

VIII. COMPARISON WITH EXPERIMENTS

Experiments measure the longitudinal and Hall resistances $R_{\alpha\beta}$ as functions of both sheet resistance and temperature. In order to compare, we obtain the normalized relative conductances defined as

$$\Delta^N\sigma_{\alpha\beta}\equiv\frac{1}{L_{00}R_0}\frac{\delta\sigma_{\alpha\beta}}{\sigma_{\alpha\beta}}, \tag{8.1}$$

where $L_{00}\equiv e^2/2\pi^2$ and $R_0=1/\sigma_{xx}$. As shown above, a logarithmic temperature dependence in these quantities can arise either from interaction corrections or from weak localization corrections. However, although two separate groups have seen such logarithmic temperature dependences,[13,14] the prefactors seem to be more universal for $\Delta^N\sigma_{xx}$, independent of sheet resistance R_0 or sample preparation for a range of R_0, but clearly disorder and sample dependent for $\Delta^N\sigma_{xy}$ in the same range of R_0. In this section, we collect all our results above to obtain the total contribution to $\Delta^N\sigma_{\alpha\beta}$ from all possible mechanisms considered above. As used in the text, superscripts ss and sj will refer to the skew scattering and side jump mechanisms, and I and WL will refer to the interaction and weak localization corrections, respectively. While the results for $\sigma_{\alpha\beta}^{ss}$ and $\delta\sigma_{xy}^{I}$ are valid for finite range strong impurity scatterings, others are evaluated within a short-range strong impurity scattering model. We have also assumed that the spin-orbit coupling is weak.

The conductivities due to skew and side jump scatterings are

$$\sigma_{xx}^{ss}=\sum_\sigma\frac{1}{2}v_{F\sigma}^2N_\sigma\tau_{tr}, \quad \sigma_{xx}^{sj}\ll\sigma_{xx}^{ss},$$

$$\sigma_{xy}^{ss}=\sigma_{xx}^{ss}\frac{\lambda_1''}{1-\lambda_1'}, \quad \sigma_{xy}^{sj}=\frac{e^2}{2\pi}\sum_\sigma \tau_{\sigma\sigma}^z g_\sigma\frac{(1-\lambda_1')}{|1-\lambda_1|^2}. \tag{8.2}$$

Quantum corrections to the conductivities due to Coulomb interaction and weak localization effects leading to a logarithmic temperature dependence are

$$\delta\sigma_{xx}^{ss,I}=L_{00}h_{xx}\ln(T\tau), \quad \delta\sigma_{xx}^{ss,WL}=L_{00}\ln(T\tau),$$

$$\delta\sigma_{xy}^{ss,I}=0, \quad \delta\sigma_{xy}^{ss,WL}=\delta\sigma_{xx}^{ss,WL}\frac{\lambda_1''}{1-\lambda_1'},$$

$$\delta\sigma_{xy}^{sj,I}=0, \quad \delta\sigma_{xx}^{sj,I}\ll\delta\sigma_{xx}^{ss,I},$$

$$\delta\sigma_{\alpha\beta}^{sj,WL}\ll\delta\sigma_{xy}^{ss,WL}. \tag{8.3}$$

The total conductivities and quantum corrections are simply

$$\sigma_{xx}=\sigma_{xx}^{ss}, \quad \sigma_{xy}=\sigma_{xy}^{ss}+\sigma_{xy}^{sj},$$

$$\delta\sigma_{xx}=\delta\sigma_{xx}^{ss,I}+\delta\sigma_{xx}^{ss,WL}, \quad \delta\sigma_{xy}=\delta\sigma_{xy}^{WL}. \tag{8.4}$$

Using these results, we obtain

$$\Delta^N\sigma_{xx}=\frac{\sigma_{xx}^{ss}}{L_{00}}\frac{\delta\sigma_{xx}^{ss,I}+\delta\sigma_{xx}^{ss,WL}}{\sigma_{xx}^{ss}}=(1+h_{xx})\ln(T\tau),$$

$$\Delta^N\sigma_{xy}=\frac{\sigma_{xx}^{ss}}{L_{00}}\frac{\delta\sigma_{xy}^{ss,WL}}{\sigma_{xy}^{ss}+\sigma_{xy}^{sj}}=\frac{1}{(1+r_{xy})}\ln(T\tau), \tag{8.5}$$

where h_{xx} defined in Eq. (5.23) is the exchange plus Hartree interaction contribution to the longitudinal conductivity and we have defined

$$r_{xy}\equiv\frac{\sigma_{xy}^{sj}}{\sigma_{xy}^{ss}} \tag{8.6}$$

as the ratio of side-jump to skew scattering contributions to the Hall conductivity. Note that r_{xy} is a nonuniversal quantity. As shown in Ref. 14, all current experiments can be understood if $h_{xx}\ll 1$ and r_{xy} is sample dependent and is allowed to vary with disorder. In particular, this means that while the skew scattering and side-jump mechanisms both contribute to the AH conductivity, the side-jump contributions to the longitudinal conductivity as well as to the weak localization corrections to the conductivity tensor are much smaller than the corresponding skew scattering contributions when the spin-orbit coupling is weak.

IX. SUMMARY AND CONCLUSION

We develop a systematic general formulation for the AHE for strong, finite range impurity scattering starting from a microscopic model of electrons in a random potential of impurities including spin-orbit coupling. In particular, we consider quantum corrections to the AH conductivity, observed in different experiments on disordered thin ferromagnetic films with apparently different results. General symmetry arguments presented here show that the e-e interaction corrections must vanish exactly, which then implies that there must be weak localization corrections in these ferromagnetic films despite the presence of large internal magnetic fields.

Our evaluations of the WL effects within a short range but strong impurity scattering lead to the normalized relative conductances given by Eq. (8.5), where the spin-orbit coupling has been assumed to be weak. These results are consistent with all experimental observations, where the difference between different experiments arise due to different contributions from skew scattering vs side-jump mechanism.

In this paper, we have only briefly mentioned the Berry phase effects. A systematic study of the Berry phase contributions to the AHE will be reported elsewhere.

ACKNOWLEDGMENTS

We thank A. Hebard, R. Misra, and P. Mitra for useful discussions on the experimental data on the Fe film. This work has been supported by the DFG-Center for Functional Nanostructures at the Karlsruhe Institute of Technology (KIT).

APPENDIX: LONG-RANGE CORRELATED POTENTIALS

For completeness, here we consider models to incorporate possible effects of small and large angle scattering.

1. Model of small angle scattering

Long-range correlated potentials will scatter electrons predominantly by a small angle $\theta \ll \pi$. A simple model is provided by a Gaussian dependence

$$V(\mathbf{k}-\mathbf{k}') = V(\theta) = 4\sqrt{\pi} V_0 \theta_0^{-1} e^{-(\theta/\theta_0)^2}, \tag{A1}$$

where $\theta_0 \ll \pi$. The angular momentum components of $V(\theta)$ are given by

$$V_m^{ns} = \int_0^{\pi} \frac{d\theta}{2\pi} V(\theta) = V_0 e^{-m^2\theta_0^2/4}. \tag{A2}$$

In the limit of weak scattering, we have $\bar{f}_{m\sigma} = \bar{V}_{m\sigma}$ and then

$$\gamma_\sigma = \sum_m |\bar{V}_{m\sigma}|^2 = (\pi N_\sigma V_0)^2 \sqrt{2\pi}/\theta_0. \tag{A3}$$

Neglecting skew scattering for the moment, we find

$$\bar{t}_{1\sigma}^{+,-} = \gamma_\sigma^{-1} (\pi N_\sigma V_0)^2 \sum_m e^{-\theta_0^2/4[m^2+(m-1)^2]} = e^{-\theta_0^2/8}. \tag{A4}$$

It follows that $1-\bar{t}_{1\sigma}^{+,-} \approx \theta_0^2/8 \ll 1$ and therefore the diffusion coefficient is enhanced by a factor

$$D/D_0 = (\theta_0^2/8)^{-1}. \tag{A5}$$

2. Model of strong backscattering

It is well known that the scattering of conduction electrons in amorphous metals can be anomalous in the sense that the transport relaxation time is smaller than the single particle relaxation time. This is due to the fact that the atomic structure is characterized by finite range order. The pair correlation function shows enhanced peaks corresponding to the nearest neighbor, next nearest neighbor, etc., shell. In other words, the system shows crystalline order over a certain usually short distance. As a consequence, electrons are suffering Bragg scattering by large angles. The scattering cross section for large angles is larger than that for small angles. Consequently, the angular average of the cross section $\sigma(\theta)$, weighted with the factor $(1-\cos\theta)$, appearing in the expression for the transport relaxation rate is larger than the uniform average in the single particle transport rate. In the case of polycrystalline material, we expect a similar effect.

The scattering potential $V(r)$ of a crystallite or a small grain of amorphous metal will show oscillating behavior in real space reflecting the nearly regular arrangement of atoms, and its Fourier transform will show a peak at a finite momentum $q=2\pi/a$ corresponding to the spatial period a, which will be equal or close to the lattice constant of the crystalline phase. The width of the peak will be determined by the range of the short-range order or the size of the crystallites. This is in contrast to a usual impurity potential whose Fourier transform has a peak at $q=0$ and a width corresponding to the range of the potential. In terms of the angular momentum components V_l of the scattering potential, a peak in $V(q)$ implies that some of the V_l will be negative. In particular, the component λ_1 of the t matrix $t_{kk'}$ determining the transport relaxation rate will be negative.

Let us consider a simple model of a crystallite of size L. Its scattering potential seen by a conduction electron of the matrix (assumed to be isotropic, as appropriate for an amorphous system) is something like

$$\begin{aligned} V_1(x) &= V_0 \cos(2\pi x/a)\theta(L/2-|x|) \\ &= V_0 S_1(x) \quad \text{one dimension}, \end{aligned}$$

$$V_2(x,y) = V_0 S_1(x) S_1(y) \quad \text{two dimensions}. \tag{A6}$$

The Fourier transform of $S_1(x)$ is given by

$$S_1(k) = \frac{L}{2}\frac{[K\cos(K)\sin(\kappa) - \kappa\sin(K)\cos(\kappa)]}{[K^2 - \kappa^2]}, \quad \text{(A7)}$$

where $K=kL/2$, $\kappa=\pi L/a$. $S_1(k)$ increases linearly with k at small k, has maximum at $k\approx 2\pi/a$, and decreases as $1/k$ for large k. We may model this behavior by

$$V_2(k) = V_0\frac{kk_0}{k_0^2 - k^2}, \quad \text{(A8)}$$

where $k_0=2\pi/a$. Using the relation of the transferred momentum $\mathbf{k}=\mathbf{k}_f-\mathbf{k}_i$ to the scattering angle ϕ, $k^2=2k_F^2(1-\cos\phi)$, where $|\mathbf{k}_{f,i}|=k_F$, we get

$$V_2(\phi) = \bar{V}\frac{\sqrt{1-\cos\phi}}{\eta + \cos\phi}, \quad \text{(A9)}$$

where $\bar{V}=V_0/(k_F\sqrt{2})$, $\eta=k_0^2/2k_F^2-1$.

The angular momentum components V_l may be calculated as

$$V_l = \int_0^{2\pi}\frac{d\phi}{2\pi}\cos(l\phi)V_2(\phi). \quad \text{(A10)}$$

In particular, we find

$$V_0 = \frac{2}{\pi}\bar{V}(\eta-1)^{-1/2}\arctan\sqrt{\frac{2}{\eta-1}} > 0,$$

$$V_1 = \frac{2}{\pi}\bar{V}\left\{-\frac{\eta}{\sqrt{\eta-1}}\arctan\sqrt{\frac{2}{\eta-1}} + \sqrt{2}\right\} \leqslant 0. \quad \text{(A11)}$$

In the limit $\eta\to 1$, the ratio of the $l=1$ and $l=0$ components is given by $V_1/V_0=-\eta$. We may estimate η by assuming Z electrons in a unit cell of area a^2 resulting in $k_F^2=2\pi Z/a^2$ and therefore $\eta=2\pi/Z-1$. For $Z\approx 2,5$ appropriate for a mixture of Fe^{2+} and Fe^{3+}, one finds $\eta\approx 1.5$ and then $V_1/V_0\approx -0.6$. In the following, we will take the V_l to be given parameters, which may be negative.

In order to keep the calculation simple, we will neglect all angular momentum components with $|l|\geqslant 2$. Defining dimensionless quantities $\bar{V}_l=\pi N_\sigma V_l$ as before, the dimensionless scattering amplitudes are given by

$$\bar{f}_0^s = \overline{V_0}/(1+is\bar{V}_0), \quad \bar{f}_{\pm 1,\sigma}^s = \bar{V}_{\pm 1,\sigma}/(1+is\bar{V}_{\pm 1,\sigma}),$$

$$\bar{V}_{\pm 1,\sigma} = \overline{V_1} \pm \sqrt{u}\tau_{\sigma\sigma}^z. \quad \text{(A12)}$$

Assuming weak spin-orbit scattering, we may expand in $\sqrt{u}$,

$$\bar{f}_{\pm 1,\sigma}^s = \frac{\overline{V_1}}{1+is\bar{V}_1} \pm (1+is\bar{V}_1)^2\sqrt{u}\tau_{\sigma\sigma}^z. \quad \text{(A13)}$$

The normalization factor γ_0 entering the expression for the relaxation rate is obtained as

$$\gamma_0 = \frac{w}{1+w} + 2\frac{w_1}{1+w_1} + O(\sqrt{u}), \quad \text{(A14)}$$

where $w=\overline{V_0}^2$, $w_1=\overline{V_1}^2$. The eigenvalue λ_1 of $t_{kk'}$ is found as

$$\lambda_1 = \frac{1}{\gamma_0}\left[\frac{2\overline{V_0}\overline{V_1}(1+\overline{V_0}\overline{V_1})}{(1+w)(1+w_1)} + 2i\sqrt{u}\tau_{\sigma\sigma}^z\overline{V_0}\frac{\overline{V_0}(1-w_1) - 2\overline{V_1}}{(1+w)(1+w_1)^2}\right]. \quad \text{(A15)}$$

Analyzing this expression, one finds that the largest negative values of λ_1 are reached for weak scattering, $\overline{V_0},\overline{V_1}\ll 1$, when

$$\lambda_1 = \frac{2\overline{V_0}}{w+w_1}[\overline{V_1} + i(\overline{V_0} - 2\overline{V_1})\sqrt{u}\tau_{\sigma\sigma}^z]. \quad \text{(A16)}$$

The minimum of λ_1' is obtained if $\overline{V_1}/\overline{V_0}=-1/\sqrt{2}$, where $\lambda_1'=-1/\sqrt{2}$.

Let us now consider diagram w_2, which is determined by the parameter $J_2^{\alpha\beta}$, given by

$$J_2^{xx} = -\gamma_0^{-1}[(1+\tilde{\lambda}_1)^2(\bar{f}_0^+\bar{f}_{+1,\sigma}^+ + \bar{f}_0^-\bar{f}_{-1,\sigma}^-) + \text{c.c.}],$$

$$b_1 \equiv \bar{f}_0^+\bar{f}_{+1,\sigma}^+ + \bar{f}_0^-\bar{f}_{-1,\sigma}^- \quad \text{(A17)}$$

$$= \frac{2\overline{V_0}}{(1+w)(1+w_1)} \times\left[\overline{V_1}(1-\overline{V_0V_1}) - i\sqrt{u}\tau_{\sigma\sigma}^z\frac{\overline{V_0}(1-w_1)+2\overline{V_1}}{(1+w_1)}\right]. \quad \text{(A18)}$$

In the weak scattering limit, we have

$$\beta_1 \equiv b_1/\gamma_0 = \frac{2\overline{V_0}}{w+w_1}[\overline{V_1} - i(2\overline{V_1}+\overline{V_0})\sqrt{u}\tau_{\sigma\sigma}^z], \quad \text{(A19)}$$

which differs from λ_1 only by the sign of the term $\bar{V}_0$ in the imaginary part, i.e., $\beta_1'=\lambda_1'$.

*muttalib@phys.ufl.edu

†woelfle@tkm.uni-karlsruhe.de

[1] R. Karplus and J. M. Luttinger, Phys. Rev. **95**, 1154 (1954); W. Kohn and J. M. Luttinger, *ibid.* **108**, 590 (1957).

[2] J. Smit, Physica (Amsterdam) **21**, 877 (1955); Phys. Rev. B **8**, 2349 (1973); N. F. Mott, Proc. R. Soc. London, Ser. A **124**, 425 (1929).

[3] L. Berger, Phys. Rev. B **2**, 4559 (1970); E. Adams and E. Blount, J. Phys. Chem. Solids **10**, 286 (1959); S. K. Lyo and T. Holstein, Phys. Rev. Lett. **29**, 423 (1972).

[4] G. Sundaram and Q. Niu, Phys. Rev. B **59**, 14915 (1999); R. Shindou and N. Nagaosa, Phys. Rev. Lett. **87**, 116801 (2001); T. Jungwirth, Q. Niu, and A. H. MacDonald, *ibid.* **88**, 207208 (2002); W.-L. Lee, S. Watauch, V. L. Miller, R. J. Cava, and N. P. Ong, Science **303**, 1647 (2004); C. Zeng, Y. Yao, Q. Niu, and H. H. Weitering, Phys. Rev. Lett. **96**, 037204 (2006).

[5] J. M. Luttinger, Phys. Rev. **112**, 739 (1958); P. Noziers and C. Lewiner, J. Phys. (Paris) **34**, 901 (1973).
[6] C. Lewiner, O. Betbeder-Matibet, and P. Nozieres, J. Phys. Chem. Solids **34**, 765 (1973).
[7] N. A. Sinitsyn, Q. Niu, and A. H. MacDonald, Phys. Rev. B **73**, 075318 (2006); N. A. Sinitsyn, A. H. MacDonald, T. Jungwirth, V. K. Dugaev, and J. Sinova, *ibid.* **75**, 045315 (2007).
[8] V. K. Dugaev, A. Crepieux, and P. Bruno, Phys. Rev. B **64**, 104411 (2001).
[9] A. Langenfeld and P. Wölfle, Phys. Rev. Lett. **67**, 739 (1991).
[10] P. Wölfle and K. A. Muttalib, Ann. Phys. **15**, 508 (2006).
[11] B. I. Altshuler and A. G. Aronov, in *Electron-Electron Interactions in Disordered Systems*, edited by A. L. Efros and M. Pollak (Elsevier, Amsterdam, 1985).
[12] P. A. Lee and T. V. Ramakrishnan, Rev. Mod. Phys. **57**, 287 (1985).
[13] G. Bergmann and F. Ye, Phys. Rev. Lett. **67**, 735 (1991).
[14] P. Mitra, R. Misra, A. F. Hebard, K. A. Muttalib, and P. Wölfle, Phys. Rev. Lett. **99**, 046804 (2007).
[15] G. Tatara, H. Kohno, E. Bonet, and B. Barbara, Phys. Rev. B **69**, 054420 (2004); M. Plihal, D. L. Mills, and J. Kirschner, Phys. Rev. Lett. **82**, 2579 (1999).
[16] M. Singh, C. S. Wang, and J. Callaway, Phys. Rev. B **11**, 287 (1975).
[17] A. A. Abrikosov, L. P. Gorkov, and I. E. Dzyaloshinski, *Methods of Quantum Field Theory in Statistical Physics* (Dover, New York, 1975).
[18] A. Crepieux, J. Wunderlich, V. K. Dugaev, and P. Bruno, J. Magn. Magn. Mater. **242**, 464 (2002).
[19] C. Zeng, Y. Yao, Q. Niu, and H. H. Weitering, Phys. Rev. Lett. **92**, 037204 (2004); G. Y. Guo, S. Murakami, T.-W. Chen, and N. Nagaosa, arXiv:0705.0409 (unpublished).
[20] A. Kamenev and A. Andreev, Phys. Rev. B **60**, 2218 (1999).
[21] R. N. Bhatt, P. Wölfle, and T. V. Ramakrishnan, Phys. Rev. B **32**, 569 (1985).